Tectonophysics, 176 (1990) 245–255
Elsevier Science Publishers B.V., Amsterdam – Printed in The Netherlands

Natural rotated inclusions in non-ideal shear

SIMON HANMER

Lithosphere and Canadian Shield Division, Geological Survey of Canada, 588 Booth Street, Ottawa, Ont. K1A 0E4 (Canada)

(Received May 23, 1989; revised version accepted November 7, 1989)

Abstract

Hanmer, S., 1990. Natural rotated inclusions in non-ideal shear. *Tectonophysics*, 176: 245–255.

Kinematic analysis of rotated winged inclusions is often couched in terms of ideal simple shear, with reference to a specific model based upon porphyroclasts of circular section. However, many natural winged inclusions are not porphyroclasts; commonly their geometries, as well as the orientation distribution of the inclusions themselves, reflect the non-ideal nature of the shearing deformation during which they formed. "Stair-stepped" sigma-shaped geometries may reflect the immaturity of a structure developed in non-ideal shear, or a mature structure developed in ideal simple shear. "Stair-stepped" delta-shaped geometries indicate that deformation approximated to ideal simple shear. "In-plane" (delta-shaped) geometries and skewed inclusion orientation distributions are indicators of non-ideal shear.

Introduction

The geometry of naturally occurring, rotated stiff inclusions is a potentially useful indicator of shear-sense in non-coaxially deformed rocks (e.g., Simpson and Schmid, 1983; Davidson, 1984; Hanmer, 1984; Hanmer and Lucas, 1985; Passchier and Simpson, 1986; Hooper and Hatcher, 1988; but see also Bell, 1985; Bell et al., 1986). The ideal behaviour of stiff or rigid inclusions in a soft, viscous matrix subjected to a shearing deformation has been considered both theoretically and experimentally. Some workers have been concerned with the rotational behaviour of round objects, such as garnet porphyroblasts (e.g., Rosenfeld, 1970; Ghosh, 1975; Dixon, 1976; Ghosh and Ramberg, 1978; Schoneveld, 1977; Powell and Vernon, 1979; Williams and Schoneveld, 1981; Vissers, 1987; Mandal and Banerjee, 1987; Masuda and Ando, 1988), while others have extended the scope of the analysis to encompass stubby, elliptical objects (e.g., Ghosh, 1977; Ghosh and Ramberg, 1976; Hanmer, 1984; Freeman, 1985, 1987; Passchier, 1987a 1988). Non-ideal shear is a component of ideal simple shear plus a component of shortening across the shear plane. Whereas many of the cited theoretical studies have considered both ideal and non-ideal shearing deformations, laboratory simulations have so far been confined to ideal simple shear (Passchier and Simpson, 1986; Van den Driessche and Brun, 1987; Jordan, 1987). Although the principles of rotational behaviour in two-dimensional (plane strain) non-ideal flows (e.g., Ghosh and Ramberg, 1976) are now well established and fairly straight-forward to apply, kinematic analysis of natural examples of rotated inclusions is still most commonly couched in terms of ideal simple shear (e.g., Simpson and Schmid, 1983; Vernon, 1987; Takagi and Ito, 1988; Saltzer and Hodges, 1988; Hooper and Hatcher, 1988).

Experiments by Passchier and Simpson (1986) and Van den Driessche and Brun (1987) elegantly simulate the deformation of a soft polycrystalline "mantle" about a rigid "core" in ideal simple shear. These experiments were specifically designed to reproduce sigma- and delta-shaped geometries (Passchier and Simpson, 1986) of porphyro-

0040-1951/90/$03.50

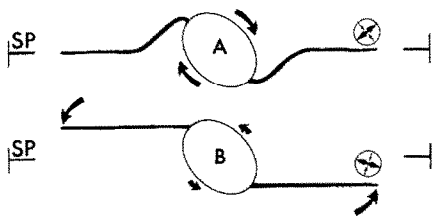

Fig. 1. The "in-plane" (*A*) and "stair-step" (*B*) geometries of two elliptical winged inclusions superficially resemble each other. However, inclusion *A* has rotated dextrally through the shear plane (SP) of the deformation. Its wings lie in a single material plane which passes through the centre of the inclusion and lies parallel to the shear plane, except immediately adjacent to the inclusion. *B* has rotated sinistrally. Its wings have rotated into the shear plane, whereas the inclusion is still markedly oblique. The structure forms a right-stepping "stair-step" wherein the wings are flats linked by the inclusion step. The lengths of the curved arrows are qualitatively proportional to rotation rates. The extensional (bold arrows) and compressional (fine arrows) quadrants of the flow are shown (see Fig. 2).

clasts and their attendant lateral appendages (wings), which commonly occur in naturally sheared rocks. Although the normalised recrystallisation rates (R/γ) used, and the finite strains attained, in the two sets of experiments are different, the structures produced have a number of features in common. Firstly, the monocrystalline core rotates faster than, and is effectively uncoupled from, the polycrystalline mantle. Secondly, the overall geometry is that of a "stair-step", wherein the attenuated mantle "flats" are linked by a "step", represented by the core, or inclusion (Fig. 1, *B*). The latter feature is observed even at high shear strains ($\gamma > 11$). However, many of the natural examples of rotated inclusions which I have observed in large-scale transcurrent ductile shear zones (Hanmer and Lucas, 1985; Hanmer, 1988a) and ductile thrust zones (Hanmer and Ciesielski, 1984; Hanmer, 1988b) are not porphyroclasts; nor are their geometries adequately explained in the context of ideal simple shear.

The aim of this contribution is to present the geometries of a variety of types of natural rotated inclusions and to examine the influence of flow strain regime on their development, in the context of a non-specific model of rotational behaviour. Discussion will be restricted to two-dimensional deformation.

Inclusions

In order to describe rotation, a frame of reference is required. The classical reference frame for flow is most familiar to geologists (Ghosh and Ramberg, 1976; cf, Ramberg, 1975; Passchier, 1987b), since it lies parallel to tangible deformation structures. Hence, in any shearing deformation, the shear plane of the deformation and its normal (N) represents the abscissa and ordinate of the reference frame (Fig. 2). Orientations (α) are measured with respect to N, in the same direction as the sense of shear. The numbered quadrants (Fig. 2) are fields of instantaneous extension (*1* and *3*) and shortening (*2* and *4*), delimited by the lines (planes in 3D) of no instantaneous longitudinal strain. The order of the quadrant numbers follows the direction of the sense of shear. All of the examples used in this contribution are taken from mylonites in well developed shear zones. Within the shear zones, transposition of pre-existing layering and the mechanical reduction of pegmatite veins to trains of isolated feldspar porphyroclasts, bear qualitative witness to the high magnitude of the shear strains involved in the deformation. Hence, all planar features in the examples can be expected to lie sub-parallel to the shear plane of the deformation. Moreover, it was possible to confirm in the field that the foliation and layering in each of the

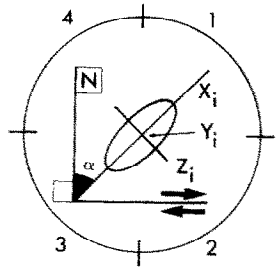

Fig. 2. Schematic representation of the kinematic reference frame for noncoaxial flow used in this paper, drawn for the special case of ideal simple shear. The instantaneous strain ellipsoid is shown (X_i, Y_i, Z_i; magnitudes of the principal instantaneous strains are exaggerated for clarity). See text.

examples lay parallel to the plane of the map-scale shear zone (Hanmer 1988a, 1988b)

Overall geometry

Consider a single stiff inclusion, with lateral appendages or wings, set in a soft viscous matrix subjected to an undefined shearing deformation. Such inclusions, monocrystalline or polycrystalline, are generally stubby and elliptical; only rarely are they circular in section (Figs. 3, 4, 5 and 7). Many inclusions are comprised of porphyroclasts of feldspar (Fig. 3), often the relics of pegmatite which has suffered extensive dynamic grain size reduction (Davidson et al., 1982; Hanmer and Ciesielski, 1984; Hanmer, 1988b; cf. Wintsch, 1975). The fine grained, polycrystalline wings attached to these inclusions may be either monomineralic feldspar or quartzo-feldspathic aggregates. Often, the wings are straight and "in-plane"; that is they lie in a single material plane which passes through the centre of the inclusion and lies parallel to the shear plane of the deformation, except for the deflection of the wings immediately adjacent to the inclusion (Figs. 1A, 3A, 3C and 7; see also Fig. 5). In other examples, the wings show a "stair-step" geometry (Figs. 1B and 3B; see also Fig. 4).

Other inclusions are polycrystalline, often polymineralic. Their wings may be deformed pressure shadows (Fig. 4), or they may be bands of matrix material, entrained by the rotating inclusion. Several of the examples of inclusions illustrated here are simply thicker segments of otherwise thin rock layers and are not necessarily rheologically distinct from their wings (Fig. 5). The important points to retain here are that a general model for the rotational behaviour of winged inclusions (1) cannot be specific to a given process of wing differentiation, (2) must account for both "stair-step" and "in-plane" geometries and (3) must allow for cases where the wings are materially continuous with the inclusion, as well as cases where the wings and the inclusion are effectively uncoupled.

A possible sequence of development stages of rotating winged inclusions is presented in Fig. 6 (see also Simpson and Schmid 1983). In Passchier and Simpson's (1986) terminology, stages *2* and *4* (Fig. 6) represent sigma-shaped and delta-shaped geometries respectively. Occasionally, stages in such a sequence can be observed in natural winged inclusions. Referring to the examples in Fig. 7, the arrested "stair-step" geometry of the immature structure (*A*) can be described in terms of two elements. The first element comprises an inclusion of moderate to low ratio, oriented with its long axis lying in the extensional quadrants of the flow at approximately $\alpha = 80°$. The second element comprises a pair of straight wings of very high aspect ratio, attached to the apices of the inclusion and oriented in the extensional quadrants of the flow at $\alpha = 85°$. Had deformation continued, example *A* would have progressed to an "S" shaped "stair-step" geometry, wherein each straight wing would be parallel to the shear plane along its length, even adjacent to the inclusion, resembling the sigma-shaped porphyroclasts of Passchier and Simpson (1986; see Fig. 6, stage *2*). Examples (*B*) and (*C*) represent more advanced stages of the same kind of structure (Fig. 7). It is important here to note that their wings lie "in-plane" and that the inclusions both lie in the compressional quadrants of the flow at α approaching 135°. They resemble the delta-shaped porphyroclasts of Passchier and Simpson (1986; see Fig. 6, stage *4*).

As the natural examples presented here illustrated, the overall geometry of many well developed winged inclusions is one of "in-plane" straight wings, deflected out of their far-field orientation in the vicinity of the inclusion, rather than that of a "stair-step" configuration. The wings of the structure may show a "stair-step" in the less mature stages of development (Fig. 6, stages *1* and *2*). The important points to note in the sequence illustrated here are that the wings rotate into the shear plane faster than the inclusion and the steps *1–3* (Fig. 6) require that the shear plane must extend in the shear direction in order to allow the wings to approach the "in-plane" configuration. Further shear strain has no effect on the orientation of the wings in the mature structure, since they are at rest in the shear plane. Only the inclusion continues to rotate forward and in doing so it deflects the proximal part of the wings (Fig. 6). Even if a finite increment of

A

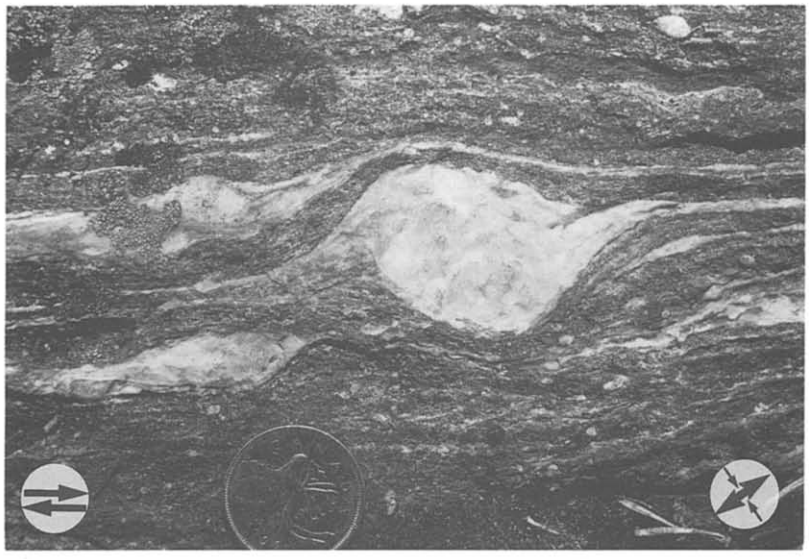

B

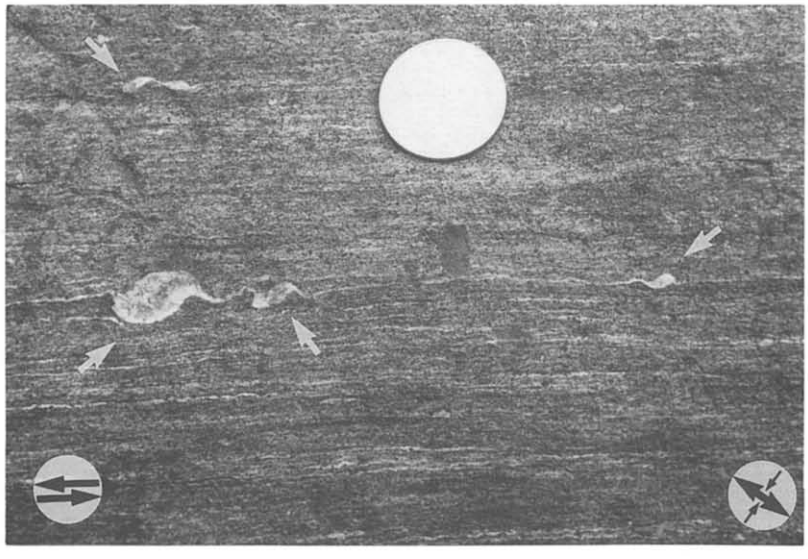

C

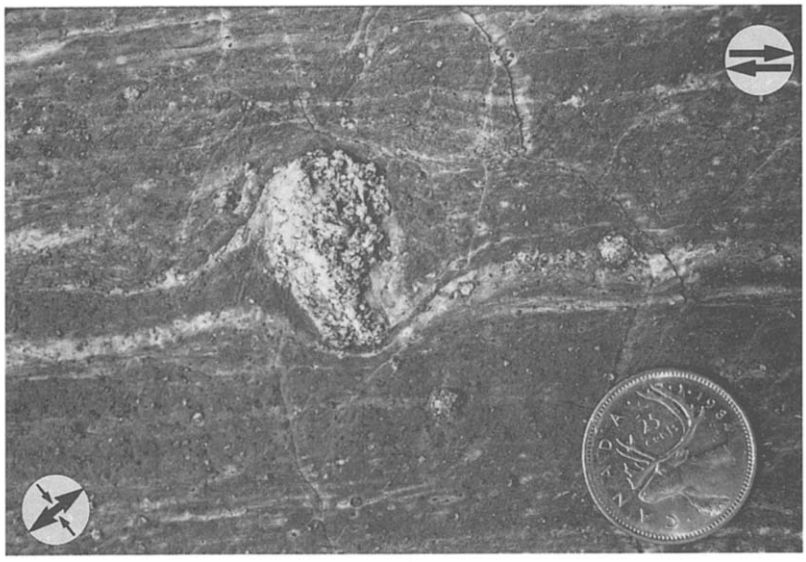

Fig. 4. Elliptical, dextrally rotated winged quartzite inclusion in a marble mylonite, observed in the *XZ* plane of the finite strain ellipsoid. Shear sense along the shear plane (parallel arrows), the extensional (bold arrows) and compressional (fine arrows) quadrants of the flow are shown. Triangular volumes of matrix were entrained between the inclusion and its wings. The white marble wings, showing a subtle left-stepping "stair-step" geometry, are composed of relatively coarse, graphite-poor material, initially formed in pressure shadows in the extensional quadrants of the flow. The pressure shadows, the right-hand one of which is particularly well preserved, have rotated toward the shear plane with progressive deformation. The proximal parts of the wings have been carried by the rotating inclusion into the compressional quadrants of the flow. Central Metasedimentary Belt, Grenville Province, Ontario (Carlson et al., 1990). Looking north-northeast.

ideal simple shear, starting with stage *3* (Fig. 6) leads to the development of stage *4* (Fig. 6), the total strain still represents a finite non-ideal shear since stage *3* implies that extension has occurred along what will eventually become the shear plane of the strain increment we are considering. The only exception is the special case of a porphyroblast which grew after the wings already lay parallel to the shear plane. The point to retain here is that "in-plane" geometries form when the entire structure is extended in the shear plane, either contemporaneously with, prior to, or after imposition of the shearing component of the deformation. Such shear-parallel extension is a condition of two-dimensional non-ideal shear (Ghosh and Ramberg, 1976). The corollary to the foregoing is that those mature winged inclusions which preserve a "stair-step" in their overall geometry must have formed in flow approximating to ideal simple shear.

Inclusion orientation

The foregoing has considered the disposition of lateral wings with respect to the inclusion and the

Fig. 3. Rotated winged feldspar porphyroclasts in mylonites, observed in the *XZ* plane of the finite strain ellipsoid. Derived by the mechanical degradation of pegmatite, qualitatively indicative of the high magnitude of the finite strain. Shear sense along the shear plane (parallel arrows), the extensional (bold arrow) and shortening (fine arrows) quadrants of the flow are shown. Note the triangular volumes of matrix entrained between the inclusion and the wings. A. The porphyroclast is circular in cross section. The wings are straight, except adjacent to the porphyroclast, and show an "in-plane" geometry. (B. The long axis of the elliptical porphyroclast lies in the compressional quadrants of the flow at $90° < \alpha < 135°$. The wings are straight, except adjacent to the porphyroclast, and show a "stair-step" geometry, stepping to the left. C. Four porphyroclasts showing geometry of Fig. 1A (arrows), derived by the mechanical degradation of granitic pegmatite in a sinistrally sheared ultramylonite. All four inclusions lie at α circa $120°$–$130°$. Note the absence of fold structures in the mylonitic foliation; the porphyroclasts are not simply the short limbs of asymmetrical folds. (A) and (B) Great Slave Lake Shear Zone, NWT (Hanmer, 1988a), (C) Parry Sound thrust zone, Grenville Province, Ontario (Davidson, 1984). Looking northeast.

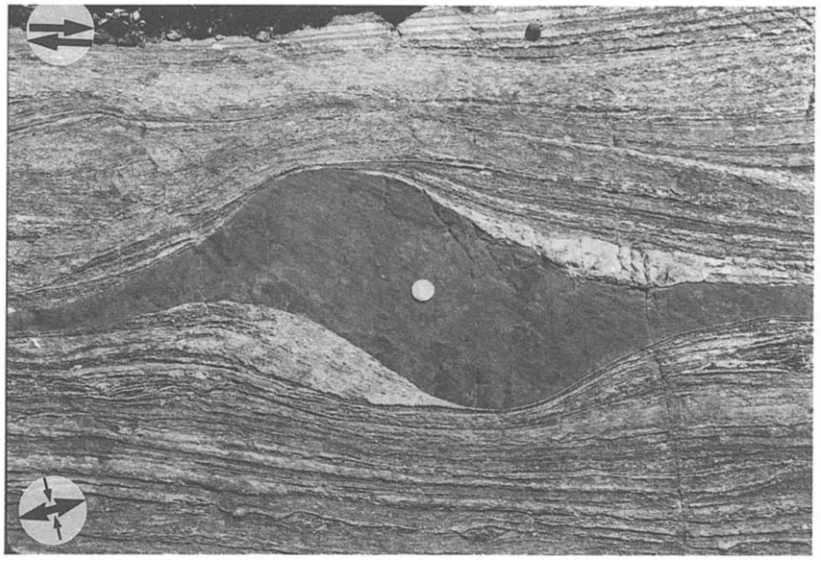

Fig. 5. A dextrally rotated "swell" in an heterogeneously extended amphibolite dyke in a mylonite matrix, observed in the *XZ* plane of the finite strain ellipsoid. Shear sense along the shear plane (parallel arrows), the extensional (bold arrows) and compressional (fine arrows) quadrants of the flow are shown. The long axis of the "inclusion" lies in the compressional quadrants of the flow, at α approaching 135. The wings are materially continuous with the 'inclusion' and show an "in-plane" geometry. Note the development of pegmatite (light grey) in the extensional quadrants of the flow, adjacent to the 'inclusion'. Great Slave Lake Shear Zone, NWT (Hanmer, 1988a). Looking down.

shear plane. Consider now the orientation of the inclusion. The long axis of the inclusion can make any angle (α) with the normal to the shear plane. However, I am struck by the frequent occurrence of field examples where the long axis of the inclusion lies within the compressional quadrants of the flow, at α approaching 135°. Given the small number of examples in any given outcrop, it is difficult to support this contention statistically. However, if valid, it is difficult to explain in the context of simple shear (Hanmer 1984; see Discussion). Quantitative support for the field-based observation is derived from the analysis of porphyroclast-bearing mylonites. Data on porphyroclasts in mylonites from the dextral transcurrent Great Slave Lake Shear Zone, Canadian Shield (Hanmer, 1986, 1988a) and from the sinistral transcurrent Median Tectonic Line, Japan (Tagaki and Ito, 1988) are presented in Fig. 8. Each population is mildly, but systematically skewed towards the compressional quadrant of the flow, such that the mode lies in the range ($90° < \alpha < 135°$). These results are encouraging. However, theory predicts that the orientations of those inclusions at rest are a partial function of the inclusion aspect ratio (Ghosh and Ramberg, 1976; Hanmer, 1984; Passchier, 1987a). Two sets of data from Great Slave Lake Shear Zone (Fig. 8E, F) do not show a detectable correlation between inclusion aspect ratio (R) and orientation (α). This presumably reflects deviation of the natural case from the ideal model due to non-Newtonian be-

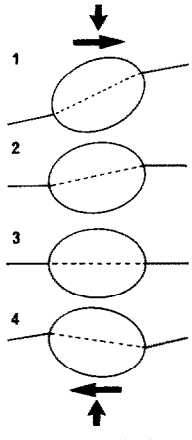

Fig. 6. A sequence of progressively developed geometries is illustrated starting with an inclusion and its wings oriented in the extensional quadrants of the flow (see Simpson and Schmid 1983), but undergoing non-ideal shear. Discussed in text.

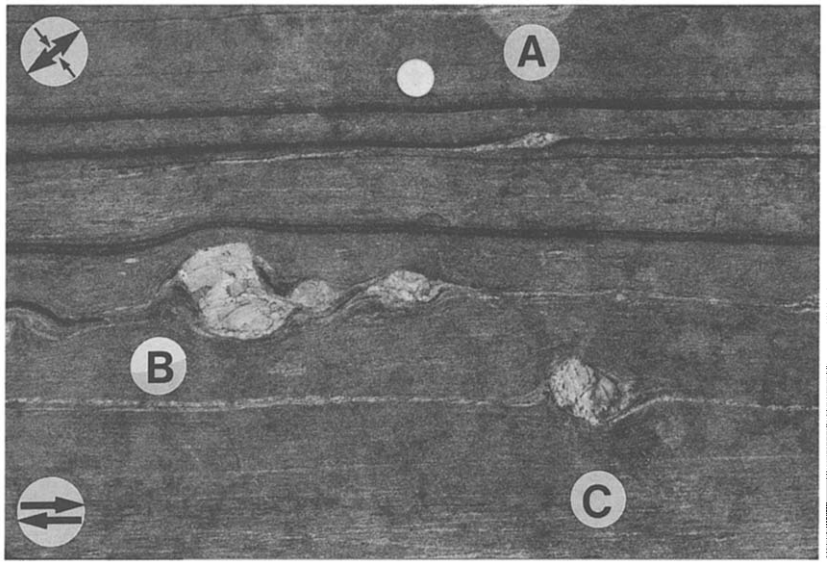

Fig. 7. Dextrally rotated winged feldspar porphyroclasts in a banded, granoblastic ultramylonite. Derived by the mechanical degradation of pegmatites, qualitatively indicative of the high magnitude of the finite strain. Observed in the XZ plane of the finite strain ellipsoid. Shear sense along the shear plane (parallel arrows), the extensional (bold arrows) and compressional (fine arrows) quadrants of the flow are shown. Both immature sigma-shapes (A) and mature delta-shaped (B and C) stages are represented. Note that in (B) and (C) the wings lie "in-plane" and that the inclusions both lie at $\alpha \sim 135°$. Discussed in text. Central Metasedimentary Belt boundary zone, Grenville Province, Quebec (Hanmer and Ciesielski, 1984). Looking down.

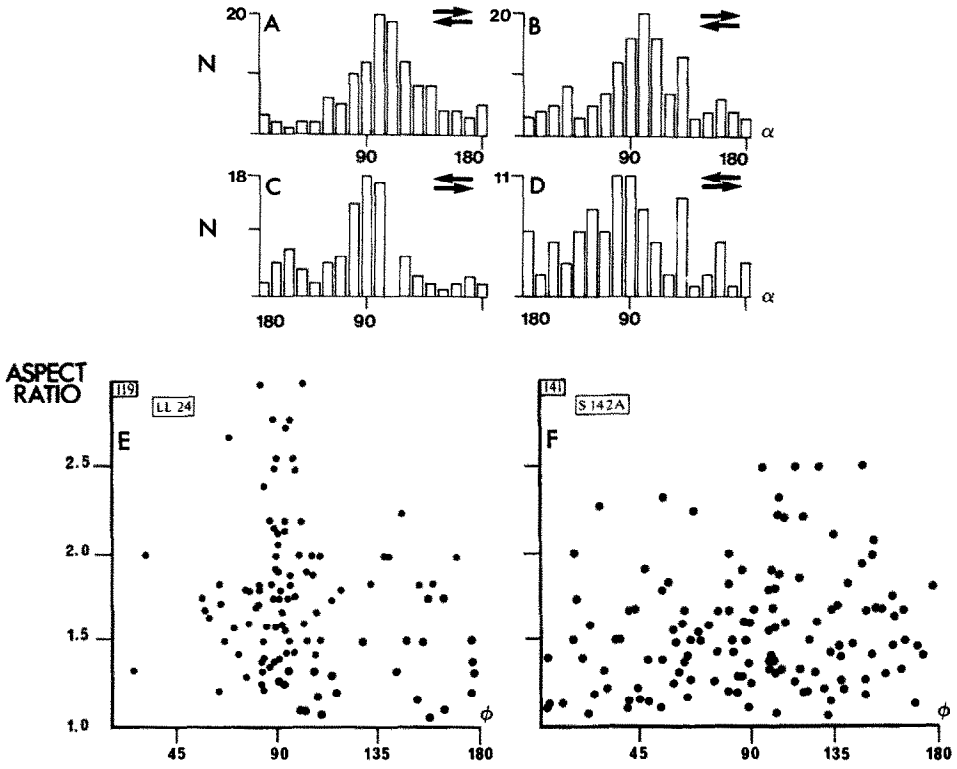

Fig. 8. (A) and (B) are data for porphyroclasts in mylonites from the dextral transcurrent Great Slave Lake Shear Zone, NWT (Hanmer 1986, 1988a). (C) and (D) are data for porphyroclasts in mylonites of the sinistral transcurrent Median Tectonic Line, Japan, taken from Tagaki and Ito (1988). Each population is mildly, but systematically skewed towards the compressional quadrant of the flow. Two sets of data from Great Slave Lake Shear Zone (E and F) do not show a detectable correlation between inclusion aspect ratio (R) and orientation (α). Discussed in text.

haviour of the matrix, deformability of the inclusions, deviation from elliptical inclusion shape and interference between inclusions. The observed break-down of the theoretical model in Fig. 8E and F calls for caution in interpreting the data sets. However, I suggest that the systematic skewness in Fig. 8A–D is significant and warrants discussion.

Rotation in shearing deformations

For clarity, it is necessary to define terms used to refer to the nature of the flow. Strain rate ratio (S_r) and the kinematical vorticity number (W_k) can both be used to describe flow in terms of the ratio of its distortional and rotational components. Each has advantages and disadvantages. The kinematical vorticity number (W_k) is a direct expression of the relationship between the rotational and distortional components of the flow, formulated in tensor notation (Means et al., 1980; Passchier, 1986). As pointed out by these authors, it is mathematically elegant and can be used to describe spinning or pulsating flows which fall outside of the pure shear–simple shear spectrum. On the other hand, the strain rate ratio is an indirect formulation couched in terms of ideal flow types (S_r = pure shear strain rate/simple shear strain rate, wherein the directions of maximum elongation rate and shear strain rate respectively of the two strain components are parallel; Ghosh and Ramberg, 1976). S_r has the anthropocentric advantage of being formulated in geologically familiar terms and I will use it throughout this discussion.

The common occurrence of asymmetrical extensional shears in shear zone rocks (e.g., Platt and Vissers, 1980; White et al., 1980) strongly suggests that many shear zones do not correspond to ideal simple shear (cf. Weijermars and Rondeel, 1984). In a constant-volume deformation, the simplest way to materially balance such extension is by shortening normal to the shear plane, in two-dimensional non-ideal shear ($S_r > 0$).

The relationship between the rotation rate of stiff inclusions and passive markers and their orientation (α) is partly a function of the strain rate ratio (S_r; Fig. 9). However, the rotation rate of an inclusion is also a function of its aspect ratio

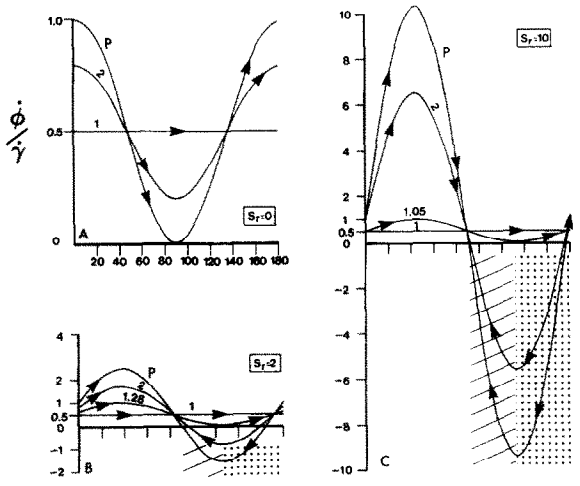

Fig. 9. Calculated curves of ideal rotational behaviour of rigid inclusions and passive markers set in a Newtonian viscous matrix for strain rate ratios (S_r) of 0 (A), 2 (B) and 10 (C). Curves are drawn for inclusions of aspect ratio (R) of 1 and 2, for inclusions of critical aspect ratio ($R_c = 1.28$ and 1.05) and for passive markers (P) in normalised rotation rate ($\dot{\phi}/\dot{\gamma}$) vs. orientation (α; measured with the sense of shear, from the shear plane normal) space. Negative values of $\dot{\phi}/\dot{\gamma}$ indicate back-rotation (arrows). Horizontal scale in B and C as in A. These idealised curves should only be taken as a guide to the behaviour of natural examples, where the inclusions may not be rigid and the matrix viscosity may not be Newtonian. Discussed in text. Modified from Ghosh and Ramberg (1976).

(R). These relationships have very important geological consequences. The rotational behaviour of inclusions and markers can be represented in terms of rotation rate ($\dot{\phi}$; normalised with respect to the shear strain rate $\dot{\gamma}$) and orientation (α) with respect to the shear plane normal (Fig. 9; Ghosh, 1975, 1977; Ghosh and Ramberg, 1976). The rotational behaviour of a rigid inclusion whose aspect ratio is greater than about 6 is essentially the same as that of a passive marker (curve P). Curves for more elongate inclusions cut the abscissa ($\dot{\phi}/\dot{\gamma} = 0$) twice, while those for stubbier inclusions do not cut it at all. Curves which graze the abscissa at a single tangent point represent inclusions of critical aspect ratio (subscript "c" as in R_c, α_c).

In any given flow, all of the rotation rate curves pass through two common cross-over or inflection points, the orientations of which are a function of the strain rate ratio (S_r). Thus in ideal simple shear ($S_r = 0$; Fig. 9A), a passive marker oriented at $0° < \alpha < 45°$ rotates faster than an equant inclusion, whereas the relative rotation rates are

inverted if the passive marker lies at $45° < \alpha < 90°$. However, compare this with the relative rotation rates for inclusions and markers at $0° < \alpha < 45°$ and $45° < \alpha < 90°$ for strongly non-ideal shear ($S_r = 10$; Fig. 9C); passive markers rotate faster than inclusions for most orientations in the extensional quadrants ($\alpha < 90°$). With increasing S_r, the curves of rotational behaviour migrate downward and toward the right, such that the left-hand rest-position ($\dot{\phi}/\dot{\gamma} = 0$) for the curve P always lies at $\alpha = 90°$ (Fig. 9). Consequently, the rotational singularity $\dot{\phi}/\dot{\gamma} = 0$ for inclusions of critical aspect ratio (R_c) migrates from α_c = circa 90° towards α_c = circa 135°, as the critical aspect ratio approaches 1. Note that in non-ideal shear inclusions rotate away from rest-positions at $\alpha > \alpha_c$ (Fig. 9 dotted field) towards rest-positions at $\alpha < \alpha_c$ (Fig. 9 rules field; Hanmer 1984).

The foregoing and Fig. 9 can be summarised as follows: In progressive ideal simple shear, all inclusions rotate with the same sense as the imposed shear (Fig. 9A). While the rotation rate for all non-circular inclusions decreases as the long axis of the inclusion approaches the shear plane, only passive markers and inclusions of high aspect ratio (curve P) come to rest ($\dot{\phi}/\dot{\gamma} = 0$) in the shear plane. Deviation from ideal simple shear ($S_r > 0$) and the migration of the curves of rotational behaviour (Fig. 9) introduces a field of back-rotation (Fig. 9B, C). Consequently, the orientation of an inclusion at rest ($\dot{\phi}/\dot{\gamma} = 0$) is a partial function of its aspect ratio. An inclusion whose long axis lies close to a potential rest position at $\alpha > \alpha_c$ tends to rotate (backwards or forwards) towards the rest position oriented at $90° < \alpha < \alpha_c$. The ideal range of occupied rest positions for a given strain rate ratio (S_r) is bounded by the left-hand rest position of curve P ($\alpha = 90°$) and the rest position of inclusions of critical aspect ratio Rc ($90° < \alpha_c < 135°$; see also Passchier, 1987a, 1988). Inclusions of aspect ratio less than R_c have no rest position and rotate continuously with the same sense as the imposed shear.

Discussion

Without attempting to apply the absolute numbers derived in Fig. 9 to natural examples, I submit that the important points to retain here are the following (1) Wings oriented in the range $45° < \alpha < 90°$ will only rotate faster than stubby inclusions oriented in the same range (Figs. 6 and 7) if the flow is non-ideal shear. (2) The distribution of rest positions occupied by inclusions in a strongly deformed matrix will only be asymmetrical with respect to the shear plane if the flow is non-ideal shear. These points guide kinematic interpretation of the natural examples illustrated in this contribution:

(a) Sigma-shaped winged inclusion geometries, *where the inclusion is elliptical*, form when the deformation path deviates from ideal simple shear. They may represent the immature stages of developing delta-shaped geometries (Figs. 6 and 7).

(b) "In-plane", delta-shaped winged inclusions indicate that the deformation path deviates from ideal simple shear (Figs. 3A and C, 5 and 7). "Stair-step", delta-shaped inclusions indicate that the deformation path is a close approximation to ideal simple shear (Figs. 3B and 4).

(c) Stubby, elliptical inclusions will tend to come to rest with their long axes oriented at α approaching 135° in strongly non-ideal shearing deformations (Figs. 3B and C, 5, 7 and 8).

Figure 9 also predicts that there should be a close correlation between the orientation (α) and the aspect ratio (R) of an inclusion. However, the data illustrated in Figs. 8E and F suggest that the theoretical model is less than perfect when applied to natural cases.

The foregoing is also pertinent to refining our understanding of the porphyroclast geometries described by Passchier and Simpson (1986) and Hooper and Hatcher (1988). The "stair-step" geometries of the sigma and delta winged porphyroclasts in the experiments of Passchier and Simpson (1986) are readily explicable in terms of ideal simple shear. However, the sigma porphyroclasts in their models are circular in section (cf. point (a) above). If they were elliptical, with the long dimension of the porphyroclast still orientated in the extensional quadrant (Simpson and Schmid 1983, fig. 4), then the relative rotation rates of the wings and the inclusion would be most readily explained in terms of non-ideal shear.

Hooper and Hatcher (1988) have recently de-

scribed wingless porphyroclasts in mylonitic rocks observed with their long dimensions oriented in the range $90° < \alpha < 135°$ (compare with Fig. 8). They have attempted to extend Passchier and Simpson's (1986) analysis to account for what they term "theta" porphyroclasts. The remarkable characteristic of theta porphyroclasts is the orientation of their long dimensions in the compressional quadrants of the flow, somewhere in the range $90° < \alpha < 135°$. However, the rationale for the kinematic significance attributed to the orientation of the inclusions is unclear since "The theta-type porphyroclast will, however, still be rotating. The characteristic non-coaxial symmetry of the regime will still be preserved..." (Hooper and Hatcher, 1988, p. 16). I submit that the stubby elliptical inclusions have come to rest at positions determined by the non-ideal nature of the flow.

In summary, the overall geometry of many natural examples of winged inclusions is independent of the process of differentiation of the wings from the inclusion. Moreover, the geometries of the rotated winged inclusions, as well as the orientation distribution of the inclusions themselves, reflect both the non-ideal nature and the sense of the shearing deformation during which they formed. "Stair-stepped" sigma-shaped geometries may reflect the immaturity of a structure developed in non-ideal shear, or a mature structure developed in ideal simple shear. "Stair-stepped" delta-shaped geometries indicate that the deformation approximated to ideal simple shear. "In-plane" (delta-shaped) geometries and skewed inclusions orientation distributions are indicators of non-ideal shear.

Acknowledgements

I am grateful to Marc St-Onge and Janet King (Geological Survey of Canada) as well as John Dixon and Wyn Means for their careful and thoughtful reviews of various versions of this paper. This is Geological Survey of Canada publication No. 35889.

References

Bell, T.H., 1985. Deformation partitioning and porphyroblast rotation in metamorphic rocks: a radical reinterpretation. J. Metamorph. Geol., 3: 109–118.

Bell, T.H., Rubenach, M.J. and Fleming, P.D., 1986. Porphyroblast nucleation, growth and dissolution in regional metamorphic rocks as a function of deformation partitioning during foliation development. J. Metamorph. Geol., 4: 37–67.

Carlson, K.A., Van der Pluijm, B.A. and Hanmer, S., 1990. Marble Mylonites near Bancroft, Ontario: evidence for crustal extension in the Canadian Grenville. Geol. Soc. Am. Bull., 102: 174–181.

Davidson, A., 1984. Identification of ductile shear zone in the southwestern Grenville Province of the Canadian Shield. In: A. Kröner and R. Greiling (Editors), Precambrian Tectonics Illustrated. Schweizerbart, Stuttgart, pp. 207–235.

Davidson, A., Culshaw, N.G. and Nadeau, L., 1982. A tectonometamorphic framework for part of the Grenville Province, Parry Sound region, Ontario. Geol. Surv. Can., Pap., 82-1A: 175–190.

Dixon, J.M., 1976. Apparent "double rotation" of porphyroblasts during a single progressive deformation. Tectonophysics, 34: 101–115.

Freeman, B., 1985. The motion of rigid ellipsoidal particles in slow flows. Tectonophysics, 113: 163–183.

Freeman, B., 1987. The behaviour of deformable ellipsoidal particles in three-dimensional slow flows: implications for geological strain analysis. Tectonophysics, 132: 297–309.

Ghosh, S.K., 1975. Distorsion of planar structures around rigid spherical bodies. Tectonophysics, 28: 158–208.

Ghosh, S.K., 1977. Drag patterns of planar structures around rigid inclusions. In: S.K. Saxena and S. Bhattacharji (Editors), Energetics of Geological Processes. Springer, Berlin, pp. 94–120.

Ghosh, S.K. and Ramberg, H., 1976. Reorientation of inclusions by combination of pure shear and simple shear. Tectonophysics, 34: 1–70.

Ghosh, S.K. and Ramberg, H., 1978. Reversal of the spiral direction of inclusion-trails in paratectonic porphyroblasts. Tectonophysics, 51: 83–97.

Hanmer, S., 1984. The potential use of planar and elliptical structures as indicators of strain regime and kinematics of tectonic flow. Geol. Surv. Can., Pap., 84-1B: 133–142.

Hanmer, S., 1986. Natural examples of the role of strain regime in the rotational behaviour or stiff inclusions. Abstr. Shear Criteria Meet., Imperial College, London, p. 12.

Hanmer, S., 1988a. Great Slave Lake Shear Zone, Canadian Shield: reconstructed vertical profile of a crustal-scale fault zone. Tectonophysics, 149: 245–264.

Hanmer, S., 1988b. Ductile thrusting at mid-crustal level, southwestern Grenville Province. Can. J. Earth Sci., 25: 1049–1059.

Hanmer, S. and Ciesielski, A., 1984. A structural reconnaissance of the northwestern boundary of the Central Metasedimentary Belt, Grenville Province, Ontario and Québec. Geol. Surv. Can., Pap., 84-1B: 121–131.

Hanmer, S. and Lucas, S.B., 1985. Anatomy of a ductile transcurrent shear: the Great Slave Lake Shear Zone, District of Mackenzie, NWT (preliminary report). Geol. Surv. Can., Pap., 85-1B: 7–22.

Hooper, R.J. and Hatcher, R.D., 1988. Mylonites from the Towaliga fault zone, central Georgia: products of heterogeneous non-coaxial deformation. Tectonophysics, 152: 1–17.

Jordan, P.G., 1987. The deformational behaviour of bimineralic limestone–halite aggregates. Tectonophysics, 135: 185–197.

Mandal, N. and Banerjee, S., 1987. Rotation rate versus growth of syntectonic porphyroblasts: the controlling parameter of the shape of the inclusion trail. Tectonophysics, 136: 165–169.

Masuda, T. and Ando, S., 1988. Viscous flow around a rigid spherical body: a hydrodynamical approach. Tectonophysics, 148: 337–346.

Means, W.D., Hobbs, B.E., Lister, G.S. and Williams, P.F., 1980. Vorticity and non-coaxialty in progressive deformations. J. Struct. Geol., 2: 371–378.

Passchier, C.W., 1986. Flow in natural shear zones—the consequences of spinning flow regimes. Earth Planet. Sci. Lett., 77: 70–80.

Passchier, C.W., 1987a. Stable positions of rigid objects in non-coaxial flow—a study in vorticity analysis. J. Struct. Geol., 9: 679–690.

Passchier, C.W., 1987b.Efficient use of the velocity gradients tensor in flow modelling. Tectonophysics, 136: 159–163.

Passchier, C.W., 1988. Analysis of deformation paths in shear zones. Geol. Rundsch., 77: 309–318.

Passchier, C.W. and Simpson, C., 1986. Porphyroclast systems as kinematic indicators. J. Struct. Geol., 8: 831–844.

Platt, J.P. and Vissers, R.L., 1980. Extensional structures in anisotropic rocks. J. Struct. Geol., 2: 397–410.

Powell, C.McA. and Vernon, R.H., 1979. Growth and rotation history of garnet porphyroblasts with inclusion spirals in a Karakoram schist. Tectonophysics, 54: 25–43

Ramberg, H., 1975. Particle paths, displacement and progressive strain applicable to rocks. Tectonophysics, 28: 1–37.

Rosenfeld, J.L., 1970. Rotated garnets in metamorphic rocks. Geol. Soc. Am., Spec. Pap., 129: 105 pp.

Saltzer, S.D. and Hodges, K.V., 1988. The Middle Mountain shear zone, southern Idaho: kinematic analysis of an early Tertiary high-temperature detachment. Geol. Soc. Am. Bull., 100: 96–103.

Schoneveld, C., 1977. A study of some typical inclusion patterns in strongly paracrystalline-rotated garnets. Tectonophysics, 39: 453–471.

Simpson, C. and Schmid, S.M., 1983. An evaluation of criteria to deduce the sense of movement in sheared rocks. Geol. Soc. Am. Bull., 94: 1281–1288.

Takagi, H. and Ito, M., 1988. The use of asymmetric pressure shadows in mylonites to determine the sense of shear. J. Struct. Geol., 10: 347–360.

Van den Driessche, J. and Brun, J.P., 1987. Rolling structures at large shear strain. J. Struct. Geol., 9: 691–704.

Vernon, R.H., 1987. A microstructural indicator of shear sense in volcanic rocks and its relationship to porphyroclast rotation in metamorphic rocks. J. Geol., 95: 127–133.

Vissers, R.L.M., 1987. The effect of foliation orientation on the inferred rotation axes and rotation angles of rotated porphyroblasts. Tectonophysics, 139: 275–283.

Weijermars, R., and Rondeel, H.E., 1984. Shear band foliation as indicator of sense of shear: field observations in central Spain. Geology, 12: 603–606.

White, S.H., Burrows, S.E., Carreras, J., Shaw, N.D. and Humphreys, F.J., 1980. On mylonites in ductile shear zones. J. Struct. Geol., 2: 175–187.

Williams, P.F. and Schoneveld, C., 1981. Garnet rotation and the development of axial plane crenulation cleavage. Tectonophysics, 78: 307–334.

Wintsch, R.P., 1975. Feldspathisation as a result of deformation. Geol. Soc. Am. Bull., 86: 35–38.